Journal of Experimental Nanoscience

ISSN: 1745-8080 (Print) 1745-8099 (Online) Journal homepage: https://www.tandfonline.com/loi/tjen20

The mechanism of oxidative damage in the nephrotoxicity of mice caused by nano-anatase TiO_2

Jingfang Zhao , Na Li , Sisi Wang , Xiaoyang Zhao , Jue Wang , Jingying Yan , Jie Ruan , Han Wang & Fashui Hong

To cite this article: Jingfang Zhao , Na Li , Sisi Wang , Xiaoyang Zhao , Jue Wang , Jingying Yan , Jie Ruan , Han Wang & Fashui Hong (2010) The mechanism of oxidative damage in the nephrotoxicity of mice caused by nano-anatase TiO_2 , Journal of Experimental Nanoscience, 5:5, 447-462, DOI: 10.1080/17458081003628931

To link to this article: https://doi.org/10.1080/17458081003628931

Published online: 05 Nov 2010.

Journal of Experimental Nanoscience
Vol. 5, No. 5, October 2010, 447–462

Taylor & Francis
Taylor & Francis Group

The mechanism of oxidative damage in the nephrotoxicity of mice caused by nano-anatase TiO_2

Jingfang Zhao†, Na Li, Sisi Wang†, Xiaoyang Zhao†, Jue Wang†, Jingying Yan, Jie Ruan, Han Wang and Fashui Hong*

Medical College of Soochow University, Suzhou 215123, P.R. China

(*Received 2 September 2009; final version received 16 January 2010*)

While the nephrotoxicity of high-dose nano-TiO_2 has been demonstrated, very little is known about the mechanism of oxidative stress to the animal kidney. In order to understand the nephrotoxicity of nano-anatase TiO_2 particles, various biochemical and chemical parameters were assayed in mouse kidneys. Abdominal exposures of high-dose nano-anatase TiO_2 caused nephritis and oxidative stress to kidney. An increase in coefficients of the kidney, Ti accumulation and histopathological changes in kidney could be observed, followed by increased reactive oxygen species generation and lipid peroxidation, and decreased activities of superoxide dismutase, catalase, ascorbate peroxidase and total antioxidant capacity as well as antioxidants such as glutathione and ascorbic acid content. In addition, kidney functions were disrupted, including increase of the creatinine, calcium and phosphonium, and reduction of uric acid and blood urea nitrogen. Our results suggest that nephritis generation in mice caused by nano-anatase TiO_2 particles is closely related to oxidative stress.

Keywords: nano-anatase TiO_2; mice; kidney; oxidative stress; nephritis

1. Introduction

Titanium dioxide (TiO_2), a natural non-silicate mineral oxide, occurs in different forms and is widely used in the cosmetic, pharmaceutical and paint industries as a colouring material [1]. However, its special characteristics such as small size, large surface per mass and high reactivity make it easy to enter into the human body and, therefore, poses potential risk to human health and the environment [2,3]. Such widespread use and its potential entry through dermal, ingestion and inhalation routes suggest that nano-titanium dioxide (nano-TiO_2) could pose an exposure risk to humans, though TiO_2 was considered to be biologically inert [4–7]. Recent investigations have unequivocally showed that exposure to nano-TiO_2 caused inflammation of the liver, kidney, spleen, lung, heart and brain as well as tumours [2,8–18]. Human polymorphonuclear leukocytes exposed to

*Corresponding author. Email: hongfsh_cn@sina.com
†These authors contributed equally to this work.

ISSN 1745–8080 print/ISSN 1745–8099 online

DOI: 10.1080/17458081003628931
http://www.informaworld.com

TiO_2 (containing 90% anatase/10% rutile, 345 and 431 nm) dust produced enhanced levels of reactive oxygen species (ROS) quantified by chemiluminescence assay [1]. Oberdörster et al. [8] have demonstrated that the physical dimensions of anatase-TiO_2 particles (20 nm) play an important role in rendering their toxicity. Furthermore, they have shown that nano-TiO_2 is able to enter into the interstitial spaces of the lung. Using a luminol-dependent chemiluminescence assay, Rahman et al. [19] reported that nano-TiO_2 produced ROS when exposed to human or rat alveolar macrophages *in vitro*. Afaq et al. [20] found that nano-TiO_2 (<30 nm) increased the number of alveolar macrophage of rats and the activities of glutathione peroxidase, glutathione reductase, 6-phosphate glucose dehydrogenase and glutathione *S*-transferase by bronchial injection. However, the levels of lipid peroxidation and hydrogen peroxide radicals were also elevated by nano-TiO_2, showing that nano-TiO_2 could induce the generation of antioxidant enzymes by cellular self-protection mechanism without decreasing free radical poisoning effect. Federici et al. [21] suggested that the gill injury of rainbow trout caused by nano-TiO_2 (crystal structure of 75% rutile and 25% anatase TiO_2, 21 nm) was closely related to the oxidative stress. Long et al. [22] showed that nano-TiO_2 stimulated ROS in brain microglia and damaged neurons *in vitro*. The enhancement of lipids peroxide in the mouse liver caused by nano-anatase TiO_2 (5 nm) likely implicated an oxidative attack that was activated by a reduction of antioxidative defence mechanism [17]. Scown et al. [23] reported that in rainbow trout, upon a single high-dose exposure of TiO_2 nanoparticles (34.2 nm, a mixture of rutile and anatase) via the bloodstream, TiO_2 was accumulated in the kidneys but had minimal effect on kidney functions.

By exposing human bronchial epithelial cells (BEAS 2B cells) to different crystal structures of TiO_2 (10 or 20 nm anatase, or 200 nm rutile forms), Gurr et al. [24] found that the anatase form of TiO_2 was much more toxic, inducing DNA damages, lipid peroxidation and micronuclei formation. Furthermore, Zhu et al. [25] showed that 10–20 nm anatase TiO_2 causes stronger cytotoxicity on CHO cells and 293T cells than does 50–60 nm anatase TiO_2, which is stronger than 50–60 nm rutile. TiO_2 can be classified into three types: anatase, rutile and amorphous. The photoactivity of anatase-type TiO_2 was greater than that of the rutile type, whereas the amorphous type did not show photocatalytic activity. Because of anatase-type TiO_2 having the greatest toxicity to cells among the three types, we set to investigate its toxicity in the mouse kidney. The previously reported studies have primarily focused on the toxicological effects of mixture nano-TiO_2, and limit to only single dose in rat or mouse. However, the toxic effects caused by a mixture nano-TiO_2 or single dose of nano-TiO_2 do not truly reflect the potential ecological and health effects of nano-TiO_2 in the environment on the whole. Thus, the toxicity of nano-TiO_2 should be evaluated similar to naturally occurring conditions.

Kidney is also equipped with an advanced defence system of enzymatic and non-enzymatic antioxidants, which are known as scavengers of ROS. Nephric injury caused by nano-TiO_2 may occur when the balance between oxidant generation and the antioxidant system is altered. In this study we researched the effect of various doses of nano-anatase TiO_2 on the mouse kidney *in vivo* after 14 days of abdominal cavity injection; the oxidative injury in the kidney was also assessed by histopathological tests, and measuring biochemical parameters of kidney functions, the generation of superoxide anion (O_2^-) and hydrogen peroxide (H_2O_2) and the level of lipid peroxidation. The intracellular levels of reduced glutathione (GSH) and the activities of various primary and

secondary antioxidant enzymes that are known to regulate cellular oxidative tone are also determined.

2. Materials and method

2.1. *Chemicals and preparation*

Nano-anatase TiO_2 was prepared via controlled hydrolysis of titanium tetrabutoxide. The details of the synthesis are as follows [26]. Colloidal titanium dioxide was prepared via controlled hydrolysis of titanium tetrabutoxide. In a typical experiment, 1 ml of Ti $(OC_4H_9)_4$ dissolved in 20 ml of anhydrous isopropanol was added dropwise to 50 ml of double distilled water adjusted to pH 1.5 with nitric acid under vigorous stirring at room temperature. Then, the temperature was raised to 60°C and kept for 6 h for better crystallisation of nano-TiO_2 particles. The resulting translucent colloidal suspension was evaporated using a rotary evaporator yielding a nanocrystalline powder. The obtained powder was washed three times with isopropanol and dried at 50°C until complete evaporation of the solvent. The (101) X-ray diffraction peak of anatase is presented in Figure 1. The sizes of particles were tested using transmission electron microscopy (TEM) and are approximately 6.9 nm (Figure 2(a)).

The Ti^{4+} content in the nano-anatase was measured by inductively coupled plasma mass spectroscopy (ICP-MS) and O, C and H contents in the nano-anatase were assayed by Elementar Analysensysteme GmbH, showing that Ti, O, C and H contents in the nano-anatase were 58.114%, 40.683%, 0.232% and 0.136%, respectively. Bulk TiO_2 (rutile) was purchased from Shanghai Chem. Co., and the average grain size was 2 μm (Figure 2(b)).

A 0.5% hydroxypropylmethylcellulose K4M (HPMC, K4M) was used as a suspending agent. Nano-anatase TiO_2 and bulk TiO_2 powder was dispersed onto the surface of 0.5%,

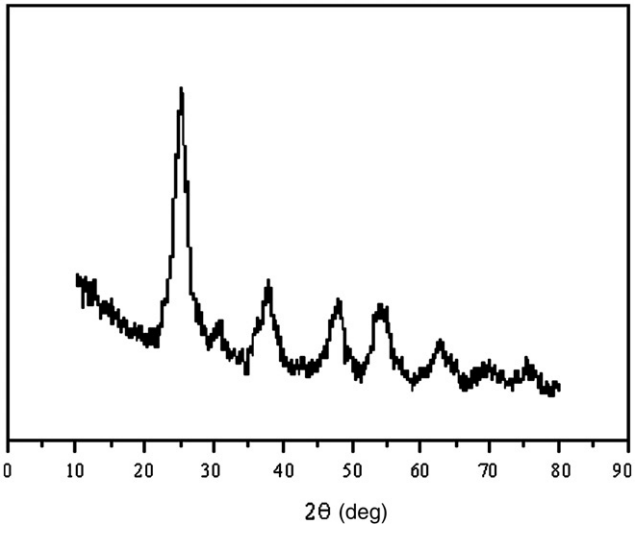

Figure 1. The (101) X-ray diffraction pattern of anatase TiO_2.

w/v HPMC, and then the suspending solutions containing nano-TiO_2 and bulk TiO_2 particles were treated by ultrasonic waves for 30 min and mechanically vibrated for 5 min.

2.2. *Animals and treatment*

CD-1 (ICR) mice (70 females, 20 ± 2 g) were purchased from the animal center of Soochow University. Animals were housed in stainless steel cages in a ventilated animal room. Room temperature was maintained at $20 \pm 2^{\circ}C$, relative humidity at $60 \pm 10\%$ and a 12 h light/dark cycle was applied. Distilled water and sterilised food for mice were available *ad libitum*. They were acclimated to this environment for 5 days prior to dosing. All procedures used in animal experiments were in compliance with the Soochow University ethics committee. Animals were randomly divided into six groups: control group (treated with 0.5% HPMC) and five experimental groups (5, 10, 50, 100, and 150 mg/kg BW nano-anatase TiO_2). Experimental groups were injected into abdominal cavity with nano-anatase TiO_2 (5, 10, 50, 100, and 150 mg/kg BW) every other day for 14 days, respectively. The control group was treated with 0.5% HPMC. The symptom and mortality were observed and recorded carefully every day for 14 days. After 14 days, the body weight of all animals were weighed and the animals were sacrificed after being anesthetised by ether. Blood samples were collected from the eye vein by removing the eyeball quickly. Serum was harvested by centrifuging blood at 2500 rpm for 10 min. The kidney was excised and weighed.

2.2.1. *Coefficients of kidney*

After weighing the body and tissues, the coefficients of kidney to body weight were calculated as the ratio of tissues (wet weight, mg) to body weight (g).

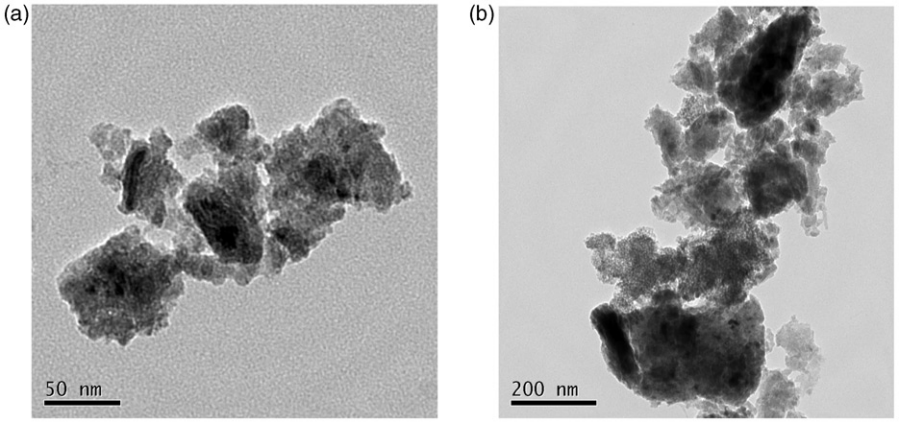

Figure 2. Sizes of TiO_2 particles observed by TEM: (a) nano-anatase TiO_2 particles and (b) bulk TiO_2 particles.

2.2.2. *Titanium content analysis of kidney*

Tissues were taken out and thawed. Approximately 0.1–0.3 g of each tissue was weighed, digested and analysed for titanium content. Briefly, prior to the elemental analysis, the tissues of interest were digested in nitric acid (ultrapure grade) overnight. After adding 0.5 ml of H_2O_2, the mixed solutions were heated at 160°C using high-pressure reaction container in an oven chamber until the samples were completely digested. Then, the solutions were heated at 120°C to remove the remaining nitric acid until the solutions were colourless and clear. At last, the remaining solutions were diluted to 3 ml with 2% nitric acid. ICP-MS (Thermo Elemental X7, Thermo Electron Co.) was used to analyse the titanium concentration in the samples. Indium (20 ng/ml) was chosen as an internal standard element. The detection limit of titanium was 0.076 ng/ml. Data are expressed as nanograms per gram of fresh tissue.

2.2.3. *Histopathological examination*

For pathological studies, all histopathological examinations were performed using standard laboratory procedures. The tissues were embedded in paraffin blocks, then sliced into 5 μm in thickness and placed onto glass slides. After hematoxylin–eosin (HE) staining, the slides were observed and the photos were taken using optical microscope (Nikon U-III Multi-point Sensor System, USA), and the identity and analysis of the pathology slides were blind to the pathologist.

2.2.4. *Biochemical analysis of kidney functions*

In this study, nephrotoxicity was determined by uric acid (UA), blood urea nitrogen (BUN), creatinine (Cr), calcium (Ca) and phosphonium (P). All biochemical assays were performed using a clinical automatic chemistry analyser (Type 7170A, Hitachi, Japan).

2.2.5. *Reactive oxygen species assay of lungs*

Superoxide ion (O_2^-) in kidney tissue was measured, as described previously by Oliveira et al. [27], by determining the reduction of 3′-{1-[(phenylamino)carbonyl]-3,4-tetrazolium}-*bis*(4-methoxy-6-nitro) benzenesulfonic acid hydrate (XTT) in the presence of O_2^-, with some modifications. The liver was homogenised with 2 ml of 50 mM Tris-HCl buffer (pH 7.5) and centrifuged at $5000 \times g$ for 10 min. The reaction mixture (1 ml) contained 50 mM Tris-HCl buffer (pH 7.5), 20 μg kidney proteins and 0.5 mM sodium, 3′-[1-[phenylamino-carbonyl]-3,4-tetrzolium]-*bis* (4-methoxy-6-nitro) benzenessulphonic acid hydrate (XTT). The reaction of XTT was determined at 470 nm for 5 min. Corrections were made for the background absorbance in the presence of 50 units of SOD. The production rate of O_2^- was calculated using an extinction coefficient of 2.16×10^4/M/cm.

The detection of H_2O_2 production in kidney tissues was carried out by flow cytometry using 2′-7′-dichlorofluoroscein diacetate (DCFH-DA; Sigma). DCFH-DA was added (10 μM final concentration) to kidney and the mixture was incubated for 30 min at 37°C. After the incubation, cells were subjected to flow cytometry analysis (FACScan; Becton Dickinson) [28].

2.2.6. *Lipid peroxidation levels assay*

Lipid peroxidation of kidneys was determined as the concentration of malondialdehyde (MDA) generated by the thiobarbituric acid (TBA) reaction, as described previously by Buege and Aust [29], with the introduction of an isobutanol extraction step for the removal of interfering compounds. For analysis, a subsample of the tissue was thawed, homogenised and cells lysed using a 4% TBA solution in 0.2 M HCl. The reaction mixture was then incubated at 90°C for 45 min. The resulting TBA–MDA adduct was phase extracted using isobutanol. The isobutanol phase was then read at a wavelength of 535 nm on a UV-3010 spectrophotometer. MDA standard curves were prepared by acid hydrolysis of 1,1,3,3-tetramethoxypropane (TMP).

2.2.7. *Antioxidant enzyme activity of kidneys*

The kidneys were homogenised in 1 ml of ice-cold 50 mM sodium phosphate (pH 7.0) containing 1% polyvinyl polypyrrolidone (PVPP). The homogenate was centrifuged at $30{,}000 \times g$ for 30 min and the supernatant was used for assays of the activities of superoxide dismutase (SOD), catalase (CAT) and ascorbic acid peroxidase (APx).

The activity of SOD was assayed by monitoring its ability to inhibit the photochemical reduction of nitroblue tetrazolium (NBT). Each 3 ml reaction mixture contained 50 mM sodium phosphate (pH 7.8), 13 μM methionine, 75 μM NBT, 2 μM riboflavin, 100 μM EDTA and 200 μl of the enzyme extract. Monitoring the increase in absorbance at 560 nm followed the production of blue formazan [30].

The CAT activity was measured by the decrease in the H_2O_2 concentration for 15 s, reading the absorbance at 240 nm on a UV-3010 absorption spectrophotometer according to Claiborne [31]. The reaction volume was 1 ml and contained 500 μl of sample homogenate and 500 μl of sodium phosphate buffer 50 mM, pH 7.0 and 15 mM H_2O_2. The control was assayed without H_2O_2. One unit of enzyme activity was defined as a decrease in the absorbance of 0.001/min at 240 nm.

APx activity was assayed using the method described by Reuveni et al. [32]. A reaction mixture consisting of 100 μl supernatant, 17 mM H_2O_2 (450 μl) and 25 mM ascorbate (450 μl) was then assayed for 3 min at 290 nm. Activity was measured as disappearance of ascorbate. One unit of enzyme activity was defined as a decrease in the absorbance of 0.001/min at 290 nm.

2.2.8. *Total antioxidant capacity of kidneys*

The assay of the total antioxidant capacity of kidneys was performed according to the manufacturer's protocols (Nanjing Jiancheng Bioengineering Institute).

2.2.9. *Glutathione and ascorbic acid assay of kidneys*

In order to perform the reduced glutathione (GSH), oxidised glutathione (GSSG) assay, the kidney was homogenised as described above. However, supernatants were not diluted fivefold as described in the case of the antioxidant enzyme assays. GSH and GSSG contents were estimated using the method of Hissin and Hilf [33]. The reaction mixture contained 100 μl of supernatant, 100 μL *o*-phthaldehyde (1 mg/ml) and 1.8 ml phosphate buffer (0.1 M sodium phosphate, 0.005 M EDTA, pH 8.0). Fluorometry was performed

using a F-4500 fluorometer (F-4500, Hitachi Co., Japan) with excitation at 350 nm and emission at 420 nm.

Kidney-reduced ascorbic acid (AsA) and dehydroascorbic acid (DAsA) determination was performed as described by Jacques-Silva et al. [34]. Protein was precipitated in 10 volumes of a cold 4% trichloroacetic acid (TCA) solution. An aliquot of homogenised sample (300 ml), in a final volume of 1 ml of the solution, was incubated at 38°C for 3°h, then 1 ml H_2SO_4 65% (v/v) was added to the medium. The reaction product was determined using colour reagent containing 4.5 mg/ml dinitrophenyl hydrazine and $CuSO_4$ (0.075 mg/ml). The content of protein was set out following the Lowry's method [35]. Each index replication was five times.

2.2.10. *Statistical analysis*

Results were analysed by analysis of variance (ANOVA). When analysing the variance treatment effect ($p \leq 0.05$); the least standard deviation (LSD) test was applied to make a comparison between means at the 0.05 levels of significance.

3. Results

3.1. *The enhancement of body weight and the coefficient of kidney*

After a 14-day treatment, the mice were sacrificed, kidneys were collected and the body weight was measured. Table 1 shows the coefficients of the kidney to body weight (wet weight of tissues)/grams (body weight). No significant differences were found in the body weight of the six groups. The significant differences were not observed in the coefficient of the kidney in the 5 and 10 mg/kg BW nano-anatase TiO_2 groups ($p > 0.05$). However, the coefficients of the kidney in the 50, 100 and 150 mg/kg BW nano-anatase TiO_2 groups and 150 mg/kg BW bulk TiO_2 group were significantly higher ($p < 0.05$ or 0.01) than the control, suggesting that high-dose nano-anatase TiO_2 and bulk TiO_2 might damage the mouse kidney.

Table 1. Increase of net weight and coefficients of the kidney of ICR mice after abdominal cavity was injected with nano-anatase TiO_2 suspensions.

	Nano-anatase (mg/kg BW)						Bulk TiO_2 (mg/kg BW)
Index	0	5	10	50	100	150	150
Net increase of BW (g)	7.86 ± 0.39	8.22 ± 0.41	7.94 ± 0.4	7.79 ± 0.39	7.46 ± 0.37	7.23 ± 0.36	7.55 ± 0.37
Kidney/BW (mg/g)	6.92 ± 0.35	6.94 ± 0.35	7.05 ± 0.35	8.38 ± 0.42*	8.59 ± 0.43*	11.18 ± 0.56**	8.61 ± 0.43*

Notes: Values represent means ± SE, $n = 10$.

Ranks marked with an asterisk or double asterisks means it is significantly different from the control (no nano-anatase or bulk TiO_2) at the 5% or 1% confidence level, respectively.

3.2. *Titanium content of kidney*

The contents of titanium in the mouse kidneys following 14 days abdominal injection to various doses of nano-anatase TiO_2 and 150 mg/kg BW bulk TiO_2 are shown in Table 2. With the injection dose of nano-anatase TiO_2 increased, the titanium accumulation in the kidney was greatly elevated. This phenomenon showed that the accumulation of titanium in the kidney was closely related to the coefficients of kidney of mice. However, the contents of titanium of the kidney in 150 mg/kg BW bulk TiO_2 group was lower than those of 150 mg/kg BW nano-anatase TiO_2 group ($p < 0.01$), suggesting that nano-anatase TiO_2 entered the kidney more easily or was much more absorbed to the kidney of mice compared with the bulk TiO_2.

3.3. *Histopathological evaluation of nephric tissue*

The histopathological changes of kidneys in the female mice are shown in Figure 3. In the 5 mg/kg BW nano-anatase TiO_2 group, the nephric tissue had no abnormal pathological changes compared with the control (Figuree 3(a) and (b)). In the 50, 100 and 150 mg/kg BW nano-anatase TiO_2 groups and 150 mg/kg BW bulk TiO_2 group, however, the significant histopathological changes were observed in the nephric tissue. For example, focal basophilia, focal stagnated blood and diffuse basophilia were shown in 50, 100 and 150 mg/kg BW nano-anatase TiO_2 groups (Figure 3(c)–(e)), respectively, and 150 mg/kg BW bulk TiO_2 group (Figure 3(f)) presented significantly stagnated blood and basophilia.

3.4. *Biochemical parameters in serum of kidney*

The changes of biochemical parameters in the blood serum of the mouse kidneys after nano-anatase TiO_2 suspension was injected into abdominal cavity are listed in Table 3. With the nano-anatase TiO_2 dose increased, the contents of Cr, Ca and P of kidney function parameters were increased gradually, although there were no statistically significant differences compared with the control group ($p > 0.05$). However, UA and BUN were decreased gradually, with the higher nano-anatase TiO_2 dosage groups being lower than the control group ($p < 0.05$ or 0.01). In the 150 mg/kg BW bulk-TiO_2 group,

Table 2. Contents of titanium in the kidneys of mice after abdominal cavity was injected with nano-anatase TiO_2 suspensions.

	Nano-anatase-TiO_2 (mg/kg BW)						Bulk TiO_2 (mg/kg BW)
Index	0	5	10	50	100	150	150
Kidney (ng/g)	80.6 ± 4.0	144.2 ± 7.2*	193.7 ± 9.7*	423.5 ± 21.1	672.7 ± 33.6*	1249.6 ± 62.5*	778.6 ± 38.9*

Notes: Values represent means ± SE, $n = 10$.

Ranks marked with an asterisk means it is significantly different from the control (no nano-anatase or bulk TiO_2) at the 5% confidence level.

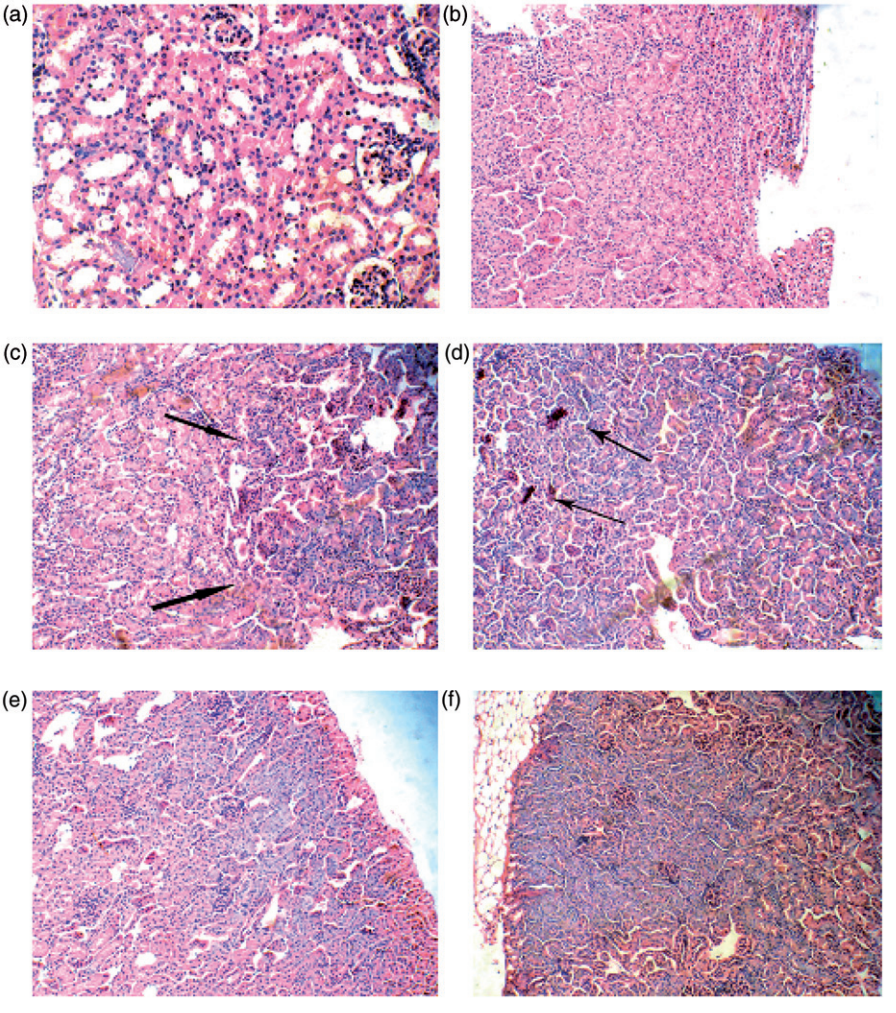

Figure 3. Histopathology of the nephric tissue in female mice after intraperitoneal injection with various doses of nano-anatase TiO_2 suspensions for consecutive 14 days. (a) control group (400×): renal glomerulus is complete and renal tubule is normal; (b) 5 mg/kg BW nano-anatase TiO_2 group (100×): without abnormal pathology changes; (c) 50 mg/kg nano-anatase TiO_2 group (200×): arrows indicate focal basophilia; (d) 100 mg/kg BW nano-anatase TiO_2 group (200×): arrows indicate focal congestion; (e) 150 mg/kg BW nano-anatase TiO_2 group (200×): diffuse basophilic degeneration and (f) 150 mg/kg BW bulk TiO_2 group (100×): obvious congestion, basophilic degeneration.

the UA and BUN were significantly lower than the control ($p < 0.05$), demonstrating that high-dose nano-anatase TiO_2 had serious toxicity to the mouse kidneys.

3.5. *ROS accumulation and lipid peroxidation of kidney*

The effects of nano-anatase TiO_2 on the generating rate of O_2^- and H_2O_2 and the MDA content in the mouse kidneys are listed in Table 4. The generating rate of O_2^- and H_2O_2

Table 3. Changes of biochemical parameters in the blood serum of mice kidneys after abdominal cavity was injected with nano-anataseTiO_2 suspensions.

	Nano-anatase (mg/kg BW)						Bulk TiO_2 (mg/kg BW)
Index	0	5	10	50	100	150	150
UA (μmol/l)	219.5 ± 10.98	223.7 ± 11.84	219.6 ± 10.98	120.7 ± 6.04**	110.3 ± 5.52**	105.2 ± 5.26**	179.5 ± 8.98*
Cr (μmol/l)	8.81 ± 0.44	8.62 ± 0.43	8.77 ± 0.44	9.13 ± 0.45	9.26 ± 0.46	9.39 ± 0.47	8.97 ± 0.45
BUN (mmol/l)	9.28 ± 0.46	9.31 ± 0.47	9.12 ± 0.45	7.71 ± 0.40*	7.45 ± 0.39*	7.31 ± 0.37*	8.16 ± 0.41*
Ca (mmol/l)	2.39 ± 0.12	2.41 ± 0.12	2.60 ± 0.13	2.68 ± 0.13	2.75 ± 0.14	2.99 ± 0.15	2.69 ± 0.13
P (mmol/l)	3.38 ± 0.17	3.40 ± 0.17	3.44 ± 0.17	3.72 ± 0.19	3.86 ± 0.19	3.92 ± 0.20	3.67 ± 0.18

Notes: Values represent means ± SE, $n = 10$.

Ranks marked with an asterisk or double asterisks means it is significantly different from the control (no nano-anatase or bulk TiO_2) at the 5% or 1% confidence level, respectively.

Table 4. Generating rate of ROS and lipid peroxidation of the kidneys of ICR mice after abdominal cavity was injected with nano-anataseTiO_2 suspensions.

Nano-anatase (mg/kg BW)	O_2^- generating rate (μmol/mg protein min)	H_2O_2 generating rate (nmol/mg protein min)	MDA content (μmol/g tissue)
0	51.60 ± 2.58	24.27 ± 1.21	7.27 ± 0.36
5	55.15 ± 2.76	24.82 ± 1.24	8.59 ± 0.43
10	58.54 ± 2.93*	29.47 ± 1.47*	13.89 ± 0.69**
50	60.05 ± 3.00*	35.49 ± 1.77**	16.15 ± 0.81**
100	85.49 ± 4.27**	55.73 ± 2.79**	22.72 ± 1.14**
150	111.60 ± 5.58**	76.08 ± 3.80**	27.06 ± 1.35**
150 Bulk TiO_2	79.15 ± 3.96*	45.96 ± 2.30*	14.07 ± 0.70**

Notes: Values represent means ± SE, $n = 10$.

Ranks marked with an asterisk or double asterisks means it is significantly different from the control (no nano-anatase or bulk TiO_2) at the 5% or 1% confidence level, respectively.

and the MDA content of the kidney in the 5 mg/kg BW nano-anatase TiO_2 groups were not significantly different from the control ($p > 0.05$), but the accumulation of ROS and the MDA content in the 10, 50, 100 and 150 mg/kg BW nano-anatase TiO_2 groups and 150 mg/kg BW bulk TiO_2 group were higher than the control ($p < 0.05$ or 0.01). Meanwhile, it can be seen from Table 4 that, the ROS accumulation and the lipid peroxidation level of kidney in the 150 mg/kg BW bulk-TiO_2 group were lower than those of 150 mg/kg BW nano-anatase TiO_2 group ($p < 0.05$).

3.6. *Defence systems of antioxidants of kidney*

The activities of antioxidative enzymatic system in the mouse kidneys caused by nano-anatase TiO_2 are presented in Table 5. With increasing the injection dose of nano-anatase TiO_2, the activities of SOD, CAT, APx and total antioxidant capacity of kidney were significantly decreased ($p < 0.05$ or 0.01), and 150 mg/kg BW bulk TiO_2 group was significantly lower than the control ($p < 0.05$ or 0.01). It is also observed from Table 5 that the enzymatic activities of kidneys caused by 150 mg/kg BW nano-anatase TiO_2 were lower than those of 150 mg/kg BW bulk TiO_2.

The defence system of non-enzymatic antioxidants in the mouse kidneys caused by nano-anatase TiO_2 is shown in Figure 4. With increasing the injection dose of nano-anatase TiO_2, the ratios of AsA to DAsA and GSH to GSSGG of kidney were gradually reduced ($p < 0.05$ or 0.01) and the reduction of the ratios of antioxidants caused by 150 mg/kg BW bulk TiO_2 was lower than those of 150 mg/kg BW nano-anatase TiO_2 ($p < 0.005$).

4. Discussion

This study suggests that intraperitoneal injection of high-dose nano-anatase TiO_2 can increase coefficients of the kidney and can be accumulated in the mouse kidneys. Further, the accumulated nano-anatase TiO_2 can induce histopathological changes of the

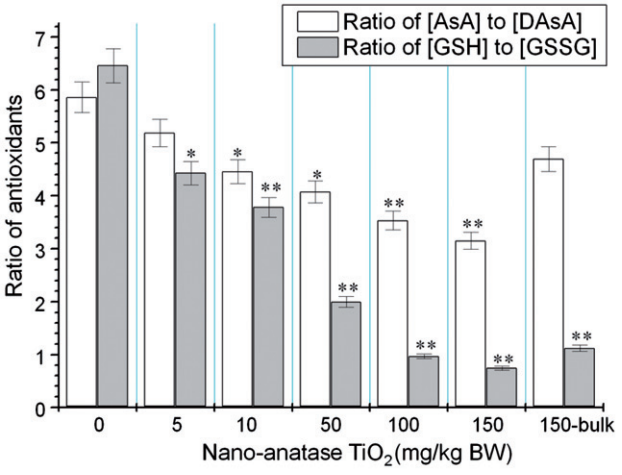

Figure 4. Ratios of AsA to DAsA and GSH to GSSGG of kidneys of mice after nano-anatase TiO_2 suspensions were injected into abdominal cavity. Note: bars marked with an asterisk or double asterisks means it is significantly different from the control (no nano-anatase or bulk TiO_2) at the 5% or 1% confidence level, respectively. Values represent means ± SE, $n = 5$.

mouse kidney, such as focal basophilia, focal stagnated blood and diffuse basophilia (Figure 3), and thus disrupts the kidney functions. Wang et al. [17] showed that there was no significant difference in the renal coefficients between experimental groups and the control, but the renal dysfunction was found in the treated mice because of the high serum BUN and Cr levels and observed the serious pathological changes of kidneys of female mice following the 2-week exposure to the 5 g/kg BW 80 nm and fine TiO_2 particles. However, Scown et al. [23] showed that even high doses of intravenously injected TiO_2 nanoparticles (34.2 nm, a mixture of rutile and anatase) caused very limited overt impairment of the renal function or oxidative stress in the blood in rainbow trout. Our current study indicates that the mouse nephrotoxicity is characteristic of the increased Cr level, the decreased BUN, UA level and pathological changes of kidneys. It is well known that serum BUN and UA were excreted out through the renal glomerulus by blood transportation and Cr is a breakdown product of creatinine phosphate and is usually produced by the body and excreted by the kidneys at a fairly constant rate [36]. The change in plasma BUN, UA and Cr concentration can be used as indicators of glomerular filtration rate, with a reduction in BUN or UA, and a rise in Cr levels indicating damage to nephrons. In this study, focal congestion and diffuse basophilic degeneration in nephric tissue were observed due to the accumulated nano-anatase TiO_2 particles, which led to the high Cr level and the low BUN, UA concentration in the serum and the serious pathological change of kidneys, and the mouse nephritis was triggered by nano-anatse TiO_2 ROS accumulation that resulted in the disruption of the nephric tissue.

One of the nano-anatase TiO_2 toxic mechanisms on kidney is an oxidative damage, probably because an imbalance between ROS and their removal damages macromolecules

and membranes, thus leading to increase of coefficients of kidney and mouse nephritis. It had been demonstrated that nano-TiO_2 particles (25 nm) stimulate ROS in BV2 microglia and are non-toxic to isolated N27 neurons, but rapidly damage neurons at low concentrations in complex brain cultures, plausibly though microglial generated ROS [22]. *In vitro* studies had also suggested that nano-TiO_2 can cause lipid peroxidation in hamster embryo fibroblast cells [24]. Our data showed that the production rate of ROS (such as O_2^- and H_2O_2) in the mouse kidney injected by higher nano-anatase TiO_2 doses was significantly elevated (Table 4), indicating that the kidney suffered from oxidative stress. Interaction between H_2O_2 and O_2^- can create OH and, $^1O_2$ which are far more destructive and can peroxidate the unsaturated lipid of the cell membrane [37]. As one kind of peroxide, MDA can intensively react with various cellular components; hence, enzymes and membranes are seriously damaged and membranous electric resistance and fluidity fall, and this eventually leads to the destruction of the membrane structure and physiological integrality [38]. In this study, the peroxidation of the kidney membrane along with nano-anatase TiO_2 dose was demonstrated by an enhancement in MDA content (Table 4). Federici et al. [21] demonstrated that TBA reactive substances showed exposure concentration-dependent and statistically significant increases in the gill, intestine and brain of rainbow trout, but not the kidney during exposure to nano-TiO_2 particles compared to controls. The effects of nano-anatse TiO_2 on lipid peroxidation in the mouse kidney could be partly explained by the direct contact of the kidney with nano-anatase TiO_2. We speculate that most of the ROS generation is from the catalytic chemical properties of nano-anatase TiO_2, which in the presence of light, can transfer electrons from substrates such as H_2O_2 to generate the hydroxyl radical. However, the effects of nano-anatase TiO_2 on ROS production may be related to the decrease of antioxidative defences *in vivo*.

Organisms use a diverse array of enzymes like SOD, CAT, and APx, as well as non-enzymatic antioxidants like ascorbate and GSH to remove oxidative stress. SOD can convert O_2^- into H_2O_2 and O_2; moreover, CAT and APx can reduce H_2O_2 into H_2O and O_2 [29,30]. Therefore, SOD, CAT and APx can keep a low level of ROS and prevent ROS from poisoning cells. Afaq et al. [20] reported that nano-TiO_2 could increase the activities of enzymatic antioxidants in alveolar macrophage, but elevate the level of lipid peroxidation and increase the accumulation of ROS. However, Liu et al. [18] proved that the activities of antioxidative enzymes from mice liver were significantly reduced, and O_2^-, H_2O and lipid peroxidation levels were elevated by higher nano-anatase TiO_2 dose. In the experiments, we also observed that the activities of SOD, CAT and APx of the kidney of mice injected by various nano-anatase TiO_2 doses were significantly inhibited (Table 5). It suggested that nano-anatase TiO_2 caused a potent oxidative stress in the kidney of mice. The reduction of enzyme activity may be related to nano-anatase TiO_2-induced inhibition of mRNA expression of SOD, CAT and APx in the mice kidneys, but it needs to be studied further. Additional evidence pointing to the possibility of an oxidative stress was provided by a reduction in ascorbate and GSH contents in the kidney injected by higher doses of nano-anatase TiO_2 (Figure 4). It indicated that nano-anatase TiO_2 accelerated ascorbic acid to be oxidised to dehydroascorbic acid, and promoted reduced glutathione (GSH) to be oxidised to oxidised glutathione in the kidney of mice. Ascorbate and GSH can directly interact with and detoxify oxygen free radicals and thus contribute significantly to non-enzymatic ROS scavenging. The depletion of ascorbate and GSH in

Table 5. Activities of antioxidative enzymes of the kidneys of ICR mice after abdominal cavity was injected with nano-anataseTiO_2 suspensions.

Nano-anatase (mg/kg BW)	SOD (U/mg protein min)	CAT (U/mg protein min)	APX (U/mg protein min)	Total antioxidant capacity (unit/mg protein)
0	33.06 ± 1.65	101.25 ± 5.06	428.57 ± 21.43	29.80 ± 1.49
5	30.25 ± 1.51	93.50 ± 4.68	414.29 ± 20.71	25.00 ± 1.25
10	28.19 ± 1.41*	55.13 ± 2.76**	360.00 ± 18.00*	23.50 ± 1.18
50	22.79 ± 1.14**	30.38 ± 1.52**	242.86 ± 12.14**	22.1 ± 1.11*
100	11.43 ± 0.57**	19.13 ± 0.96**	142.86 ± 7.14**	11.20 ± 0.56**
150	4.59 ± 0.23**	10.00 ± 0.50**	107.14 ± 5.36**	7.62 ± 0.38**
150 bulk TiO_2	15.44 ± 0.77**	27.50 ± 1.38**	271.43 ± 13.57*	15.50 ± 0.78**

Notes: Values represent means ± SE, $n = 10$.

Ranks marked with an asterisk or double asterisks means it is significantly different from the control (no nano-anatase or bulk TiO_2) at the 5% or 1% confidence level, respectively.

the kidney was associated with increases in ROS and MDA, suggesting that the kidney was using up antioxidant defences to prevent oxidative stress.

The experimental study also showed that the coefficients of the kidney, BUN concentration, ROS accumulation, lipid peroxidation level and the decrease of antioxidative systems of the kidney in the 150 mg/kg BW bulk TiO_2 group were lower than those of 100 and 150 mg/kg BW nano-anatase TiO_2 groups ($p < 0.05$), showing that nano-anatase TiO_2 has more severe toxicity to mice compared with bulk TiO_2. The discrepancy may be attributable to the grain size and total surface of nano-anatase TiO_2 and bulk-TiO_2.

5. Conclusion

The results of this study added to a growing body of knowledge of nano-anatase TiO_2-induced kidney toxicity and antioxidative responses in the mouse kidney. We suggested that high-dose nano-anatase TiO_2 could cause obvious ROS accumulation, lipid peroxidation, which was attributed to the decrease of antioxidative defence, resulting in serious nephritis.

Acknowledgements

This work was supported by the National Natural Science Foundation of China (Grant no. 30901218), the Medical Development Foundation of Suzhou University (Grant no. EE120701) and the National Bringing New Ideas Foundation of Student of China (Grant no. 57315427, 57315927).

References

[1] M. Hedenborg, *Titanium dioxide induced chemiluminescence of human polymorphonuclear leukocytes*, Int. Arch. Occup. Environ. Health 61 (1988), pp. 1–6.

[2] G. Oberdörster, E. Oberdörster, and J. Oberdörster, *Nanotoxicology: An emerging discipline evolving from studies of ultrafine particles*, Environ. Health Persp. 113 (2005), pp. 823–839.
[3] D.B. Warheit, R.A. Hoke, C. Finlay, E.M. Donner, K.L. Reed, and C.M. Sayes, *Development of a base of toxicity tests using ultrafine TiO_2 particles as a component of nanoparticle risk management*, Toxicol. Lett. 171 (2007), pp. 99–110.
[4] J. Ferin and G. Oberdörster, *Biological effects and toxicity assessment of titanium dioxides; anatase and rutile*, Am. Ind. Hyg. Assoc. J. 46 (1985), pp. 69–72.
[5] R.C. Lindenschmidt, K.E. Driscoll, M.A. Perkins, J.M. Higgins, J.K. Mourer, and K.A. Belfiore, *The comparison of a fibrogenic and two non-fibrogenic dusts by bronchoalveolar lavage*, Toxicol. Appl. Pharmacol. 102 (1990), pp. 268–281.
[6] E.M. Ophus, L.E. Rode, B. Gylseth, G. Nicholson, and K. Saeed, *Analysis of titanium pigments in human lung tissue*, Scand. J. Work Environ. Health 5 (1979), pp. 290–296.
[7] L.E. Rode, E.M. Ophus, and B. Glyseth, *Massive pulmonary deposition of rutile after titanium dioxide exposure*, Arch. Pathol. Microbiol. Scand. Sect. A 89 (1981), pp. 455–461.
[8] G. Oberdörster, J. Ferin, R. Gelein, S.C. Soderholm, and J. Finkelstein, *Role of the alveolar macrophage in lung injury: Studies with ultrafine particles*, Environ. Health Persp. 97 (1992), pp. 193–199.
[9] K.E. Driscoll, J.K. Maurer, R.C. Lindenschmidt, D. Romberger, S.I. Rennard, and L. Crosby, *Respiratory tract responses to dust: Relationships between dust burden, lung injury, alveolar macrophages fibronectin release, and the development of pulmonary fibrosis*, Toxicol. Appl. Pharmacol. 106 (1990), pp. 88–101.
[10] L.L. Ma, J. Liu, N. Li, J. Wang, Y.M. i Duan, J.Y. Yan. H.T. g. Liu, H. n Wang, F.S. Hong, *Oxidative stress in the brain of mice caused by translocated nanoparticulate TiO_2 delivered to the abdominal carity*. Biomaterials 31 (2010), pp. 99–105.
[11] J. Ferin, G. Oberdörster, S.C. Soderholm, and R. Gelein, *Pulmonary tissue access of ultrafine particles*, J. Aerosol. Med. 4 (1991), pp. 57–68.
[12] H.W. Chen, S.F. Su, C.T. Chien, W.H. Lin, S.L. Yu, C.C. Chou, J.W. Chen Jeremy, and P.C. Yang, *Titanium dioxide nanoparticles induce emphysema-like lung injury in mice*, FASEB J. 20 (2006), pp. 1732–1741.
[13] J.S. Brown, K.L. Zeman, and W.D. Bennett, *Ultrafine particle deposition and clearance in the healthy and obstructed lung*, Am. J. Respir. Crit. Care Med. 166 (2002), pp. 1240–1247.
[14] W.G. Kreyling, M. Semmler, F. Erbe, P. Mayer, S. Takenaka, H. Schulz, G. Oberdörster, and A. Ziesenis, *Translocation of ultrafine insoluble iridium particles from lung epithelium to extrapulmonary organs is size dependent but very low*, J. Toxicol. Environ. Health. A 65 (2002), pp. 1513–1530.
[15] G. Oberdörster, Z. Sharp, V. Atudorei, A. Elder, R. Gelein, W. Kreyling, and C. Cox, *Translocation of inhaled ultrafine particles to the brain*, Inhal. Toxicol. 16 (2004), pp. 437–445.
[16] J. Muller, F. Huaux, N. Moreau, P. Misson, J.F. Heilier, M. Delos, M. Arras, A. Fonseca, J.B. Nagy, and D. Lison, *Respiratory toxicity of multi-wall carbon nanotubes*, Toxicol. Appl. Pharmacol. 207 (2005), pp. 221–231.
[17] J.X. Wang, G.Q. Zhou, C.Y. Chen, H.W. Yu, T.C. Wang, Y.M. Ma, G. Jia, Y.X. Gao, B. Li, J. Sun, Y.F. Li, F. Jia, Y.L. Zhaso, and Z.F. Chai, *Acute toxicity and biodistribution of different sized titanium dioxide particles in mice after oral administration*, Toxicol. Lett. 168 (2007), pp. 176–185.
[18] H.T. Liu, L.L. Ma, J.F. Zhao, J. Liu, J.Y. Yan, J. Ruan, and F.S. Hong, *Toxicity of nano-anatase TiO_2 to mice: Liver injury, oxidative stress*, Toxicol. Environ. Chem. 92 (2010), pp. 175–186.
[19] Q. Rahman, J. Norwood, G. Oberdörster, and G. Hatch, *Rat-human differences in macrophage oxidant production by pollutant particles,* Colloquium on Particulate Air Pollution and Human Mortality and Morbidity, January, Irvine, CA, 1994, pp. 24–25.

[20] F. Afaq, P. Abidi, R. Matin, and Q. Rahman, *Cytotoxicity, pro-oxidant effects and antioxidant depletion in rat lung alveolar macrophages exposed to ultrafine titanium dioxide*, J. Appl. Toxicol. 18 (1998), pp. 307–312.

[21] G. Federici, B.J. Shaw, and R.D. Handy, *Toxicity of titanium dioxide nanoparticles to rainbow trout (Oncorhynchus mykiss): Gill injury, oxidative stress, and other physiological effects*, Aquat. Toxicol. 84 (2007), pp. 415–430.

[22] T.C. Long, J. Tajuba, P. Sama, N. Sale, C. Swartz, J. Parker, S. Hester, G.V. Lowry, and B. Veronesi, *Nano-TiO_2 stimulates ROS in brain microglia and damages neurons in vitro*, Environ. Health Persp. 115 (2007), pp. 1631–1637.

[23] T.M. Scown, R.Y. van Aerle, B.D. Johnston, S. Cumberland, J.R. Lead, O. Richard, and C.R. Tyler, *High doses of intravenously administered titanium dioxide nanoparticles accumulate in the kidneys of rainbow trout but with no observable impairment of renal function*, Toxicol. Sci. 109 (2009), pp. 372–380.

[24] J.R. Gurr, A.S.S. Wang, C.H. Chen, and K.Y. Jan, *Ultrafine titanium dioxide particles in the absence of photoactivation can induce oxidative damage to human bronchial epithelial cells*, Toxicol. 213 (2005), pp. 66–73.

[25] R.R. Zhu, S.L. Wang, J. Chao, D.L. Shi, R. Zhang, X.Y. Sun, and S.D. Yao, *Bio-effects of nano-TiO_2 on DNA and cellular ultrastructure with different polymorph and size*, Mat. Sci. Eng. C 29 (2009), pp. 691–696.

[26] P. Yang, C. Lu, N. Hua, and Y. Du, *Titanim dioxide nanoparticles co-doped with Fe^{3+} and Eu^{3+} ions for photocatalysis*, Mater. Lett. 57 (2002), pp. 794–801.

[27] C.P. Oliveira, F.P. Lopasso, F.R. Laurindo, R.M. Leitao, and A.A. Laudanna, *Protection against liver ischemia-reperfusion injury in rats by silymarin or verapamil*, Transplant. Proc. 33 (2001), pp. 3010–3014.

[28] N. Asatiani, N. Sapojnikova, M. Abuladze, T. Kartvelishvili, N. Kulikova, E. Kiziria, E. Namchevadze, and H.Y. Holman, *Effects of Cr(VI) long-term and low-dose action on mammalian antioxidant enzymes (an in vitro study)*, J. Inorg. Biochem. 98 (2004), pp. 490–496.

[29] J.A. Buege and S.D. Aust, *Microsomal lipid peroxidation*, Methods Enzymol. 52 (1978), pp. 302–310.

[30] C. Beauchamp and I. Fridovich, *Superoxide dismutase: Improved assays and assay applicable to acrylamide gels*, Anal. Biochem. 44 (1971), pp. 276–286.

[31] A. Claiborne, *Catalase activity,* in *Handbook of Methods for Oxygen Free Radical Research*, R.A. Greenwaid, ed., CRC, Boca Raton, FL, 1985, p. 283.

[32] R. Reuveni, M. Shimoni, Z. Karchi, and J. Kuc, *Peroxidase activity as a biochemical marker for resistance of muskmelon (Cucumis melo) to seudoperno spora cubensis*, Phytopathol. 82 (1992), pp. 749–753.

[33] P.J. Hissin and R. Hilf, *A fluorometric method for determination of oxidized and reduced glutathione in tissues*, Anal. Biochem. 74 (1976), pp. 214–226.

[34] M.C. Jacques-Silva, C.W. Nogueira, L.C. Broch, E.M. Flores, and J.B.T. Rocha, *Diphenyl diselenide and ascorbic changes deposition of selenium and ascorbic in liver and brain of mice*, Pharmacol. Toxicol. 88 (2001), pp. 119–125.

[35] O.H. Lowry, N.J. Rosebrough, A.L. Farr, and R.J. Randall, *Protein measurement with the folin phenol reagent*, J. Biol. Chem. 193 (1951), pp. 265–275.

[36] C.E. Bond, *Biology of Fishes*, 2nd ed., Saunders College Publishing, Orlando, FL, 1996.

[37] I. Fridovich, *The biology in oxygen radical*, Science 201 (1978), pp. 875–880.

[38] G. John, J.G. Scandalios, *Oxygen stress and superoxide dismutase*. Plant Physiol. 101 (1993), pp. 7–12.